

Optimal timing of SPECT/CT to demonstrate parathyroid adenomas in ^{99m}Tc-sestamibi scintigraphy

Kate Hunter^{ORCID}, Niamh Gavin, Colin McQuade^{ORCID}, Brendan Hogan, John Feeney
 Tallaght University Hospital, Dublin, Ireland

[Received: 26 V 2021; Accepted: 22 VI 2022]

Abstract

Background: Accurate preoperative localisation of the parathyroid adenoma is essential to achieve a minimally invasive parathyroidectomy. The purpose of this study was to validate and improve our single-isotope dual-phase parathyroid imaging protocol utilising ^{99m}Technetium-Sestamibi ([^{99m}Tc]MIBI). There has been no accepted gold standard evidence-based protocol regarding timing of single-photon emission computed tomography/computed tomography (SPECT/CT) acquisition in parathyroid imaging with resultant variation between centres. We sought to determine the optimum timing of SPECT/CT post administration of [^{99m}Tc]MIBI in the identification of parathyroid adenomas. We aimed to evaluate the efficacy of early and late SPECT/CT and to establish whether SPECT/CT demonstrates increased sensitivity over planar imaging.

Material and methods: A sample of 36 patients with primary hyperparathyroidism underwent planar and SPECT/CT acquisition 15 minutes (early) and two hours (late) post [^{99m}Tc]MIBI administration. Two radionuclide radiologists reviewed the images and Fisher's exact Chi-squared statistic was used to evaluate the diagnostic performances of early versus late SPECT/CT acquisition and SPECT/CT versus planar imaging.

Results: Twenty-one likely parathyroid adenomas were identified with a statistically superior diagnosis rate in the late SPECT/CT acquisition compared with both early SPECT/CT and planar imaging ($p < 0.05$). All adenomas diagnosed on early SPECT/CT acquisition were also identified on late SPECT/CT images.

Conclusions: Single late phase SPECT/CT is significantly superior to early SPECT/CT in the identification of parathyroid adenomas. Late SPECT/CT improves diagnostic accuracy over planar acquisition. Imaging protocols should be revised to include late SPECT/CT acquisition. Early SPECT/CT acquisition can be eliminated from scan protocols with associated implications regarding reduced scan time and increased patient throughput.

KEY words: parathyroid scintigraphy; [^{99m}Tc]MIBI; sestamibi; SPECT/CT

Nucl Med Rev 2022; 25, 2: 89–94

Introduction

Untreated primary hyperparathyroidism can result in significant morbidity including renal calculi, osteoporosis and hypercalcaemia-related complications [1]. Lifetime risk of primary hyperparathyroidism (PHPT) is estimated at 1% with up to 80% of cases due to the presence of a solitary parathyroid adenoma and less common causes including glandular hyperplasia and carcinoma [2].

For asymptomatic PHPT, medical management and conservative treatment are possible, however, surgical removal of hyperfunctioning parathyroid tissue remains the only definitive treatment [3].

Historically, the gold standard for parathyroidectomy was invasive surgery, with bilateral neck exploration necessary to locate all four parathyroid glands. Today, focused parathyroidectomy is the preferred surgical approach, made possible by pre-operative localization. Accuracy of localization is crucial to ensure successful targeted and minimally invasive surgery [4, 5]. Technetium-99m labeled sestamibi ([^{99m}Tc]MIBI) scintigraphy is the imaging agent of choice with reported sensitivities of up to 90% in accurately localizing a solitary parathyroid adenoma [6]. Planar imaging is increasingly supplemented with hybrid SPECT/CT for three-dimensional representation and anatomical localization.

Correspondence to: Kate Hunter, Tallaght University Hospital, Dublin, Ireland, phone: +35314143745, fax: +35314149805, e-mail: hunterk@tcd.ie

Dual phase imaging including early and late phase acquisition exploits the premise of differential washout of [^{99m}Tc]MIBI, with rapid wash-out from thyroid tissue and late phase retention of [^{99m}Tc]MIBI in a parathyroid adenoma [7]. However, this pattern does not occur in approximately 25% of cases raising the potential for false-negative studies [8]. False-positive results are caused by thyroid nodules, thyroiditis, and metastatic cervical lymph nodes potentially retaining [^{99m}Tc]MIBI [9]. The detection of smaller parathyroid adenomas, multiple adenomas, and parathyroid hyperplasia also poses a challenge. It has been suggested that variable uptake of [^{99m}Tc]MIBI by parathyroid adenomas is related to the number of mitochondria present in the abnormal tissue [10]. Proposed explanations for the absence of increased radiotracer uptake include multidrug resistance-associated protein and a relatively lower proportion of oxyphil cells [11].

The addition of computed tomography (CT) to gamma camera installations provides accurately localized functional and anatomical information with improved sensitivity and specificity [12].

The use of SPECT and or SPECT/CT and the timing of such acquisitions can differ greatly. Imaging protocols vary widely with significant differences in methodology between nuclear medicine departments. There is no single accepted generic protocol for parathyroid scintigraphy using SPECT/CT. In this study, we aimed to determine the optimum timing of SPECT/CT in the identification of parathyroid adenomas.

The study objective was to validate and improve local single isotope dual-phase parathyroid imaging protocols utilizing [^{99m}Tc]MIBI. We sought to establish if there is any significant difference between early and late SPECT/CT imaging in the detection and localization of parathyroid adenomas. We also wished to determine if SPECT/CT leads to improved sensitivity in the diagnosis of parathyroid adenomas when used as an adjunct to planar parathyroid scintigraphy.

Material and methods

Inclusion criteria

A prospective consecutive sampling method was employed over a 6 month period among patients who presented to our institution for investigation of PHPT. Patients were injected with [^{99m}Tc]MIBI 740 MBq (0.02 Curie) with an accepted tolerance range of 666–777 MBq (0.018–0.021 Curie). The patients were imaged on either a Siemens Symbia T2 or a Symbia T16, with a scanner chosen according to availability at the time of patient presentation. The same scanner was used for both early and late phase acquisition on a single patient in order to minimize intra-subject variability.

Acquisition protocol and scan parameters

The patient was positioned supine with a scan field of view extending from the superior orbital margin to the superior heart border. An initial planar image was acquired with a cobalt marker positioned at the sternal notch to provide an anatomical reference point. The marker was removed for subsequent planar acquisitions. Early planar acquisitions were commenced fifteen minutes post intravenous administration of [^{99m}Tc]MIBI, followed by the early SPECT acquisition. Late planar acquisitions were acquired two

hours post-administration of [^{99m}Tc]MIBI, followed immediately by late SPECT/CT.

Planar image acquisition

All patients were provided with water to drink immediately prior to early planar acquisition in order to minimize [^{99m}Tc]MIBI salivary gland activity. Planar images were acquired using the anterior camera of a dual-headed gamma camera, positioned with minimal possible distance from the patient and a low energy high resolution parallel (LEGR) collimator. The initial acquisition with the cobalt marker at the sternal notch was terminated after 100 kilocounts had been achieved with the image matrix fixed at 128 × 128. Early (15 minutes post-injection) planar images were acquired using an image matrix of 256 × 256 and images were acquired over a fixed time frame of ten minutes. Late (two hours post-injection) planar acquisition was performed over a fixed time frame of fifteen minutes.

SPECT and SPECT/CT image acquisition

A SPECT acquisition was obtained immediately following the fifteen-minute planar acquisition with an unchanged patient position with the field of view extending from the angle of the mandible to the mediastinum. A second SPECT/CT acquisition was performed following the delayed planar acquisition in all patients. Scan parameters are outlined in Table 1.

Image processing

Images were processed on Symbia.net using manufacturer software. The early SPECT acquisition and the B30 attenuated corrected CT reconstructed images were manually fused to produce early and late SPECT/CT datasets for comparative review. Multiplanar reconstructions (axial, coronal, and sagittal) were generated for both the early and late SPECT/CT acquisitions with soft tissue CT windows applied, and all images were displayed using the 'warm

Table 1. SPECT and CT acquisition parameters

Spect acquisition parameters	CT acquisition parameters	
	Topogram	CT
M: 128 × 128	mA: 25	Effective mAs: 15 CARE dose 4D
Detectors: both	kV: 130	kV: 130
Patient orientation: head out, supine	Scan time: 0.8 s	Scan time: 12.9 s
Rotation direction: clockwise	Slice thickness: 0.6 mm	Slice thickness: 5 mm Acquisition: 16 × 1.2 mm
Degrees rotation: 180	Topogram length: 512 mm	Pitch: 0.8
Number of views: 32	Tube position: top	Rotation time: 0.6 s
Time per view: 25 s		Scan delay: 3 s
Detector configuration: 180		CTDIvol: 1.68 mGy
Orbit: non-circular		
Mode: step and shoot		

CT — computed tomography; kV — kilovolt; mA — milliamperes; mGy — milligray; M — matrix; SPECT — single-photon emission computed tomography

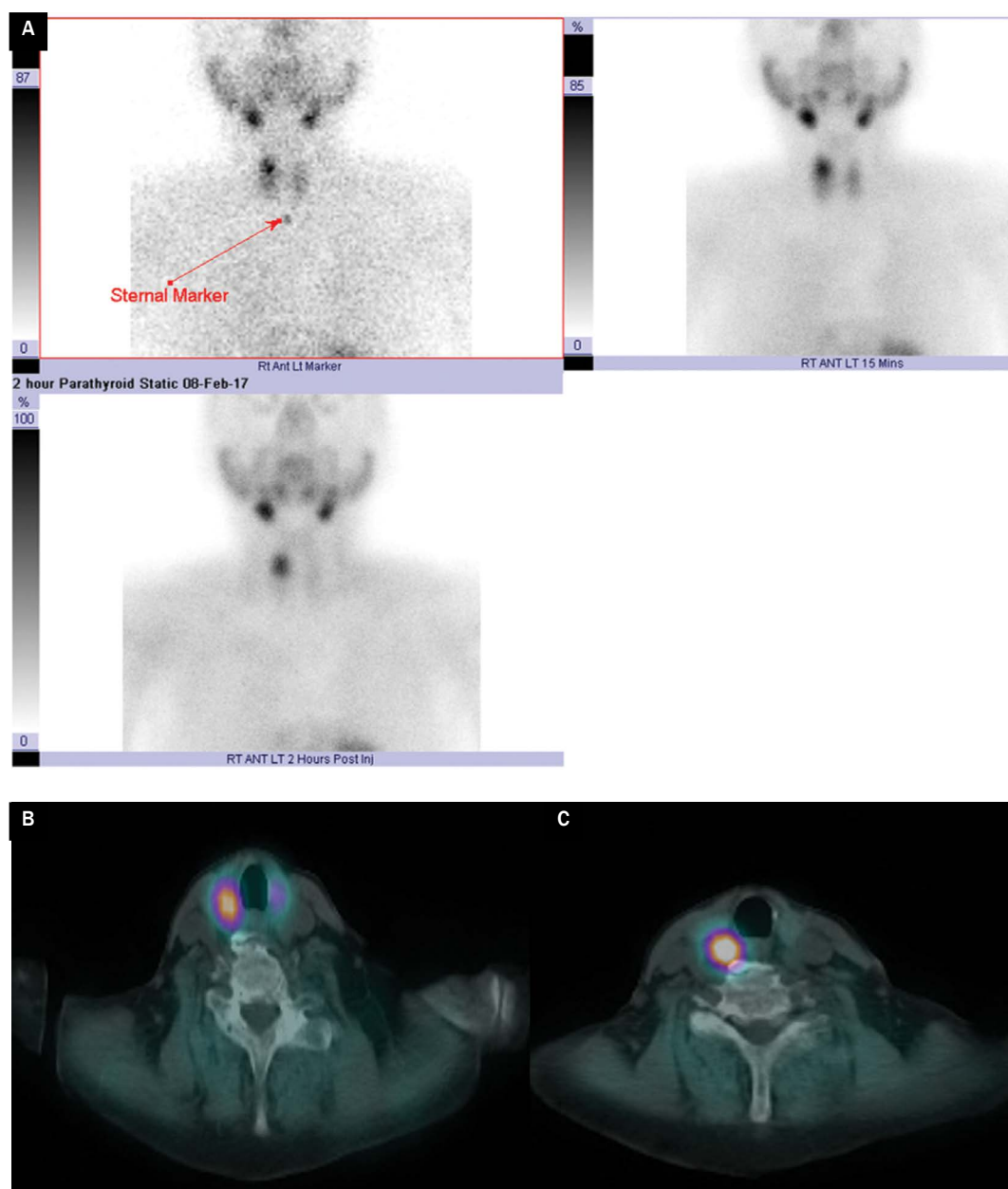


Figure 1. (A) Early and late planar images demonstrating a solitary region of [^{99m}Tc]MIBI uptake on delayed imaging indicating the presence of a parathyroid adenoma; (B) Single slice from early (15 mins) and late [(C), 2 hours] SPECT/CT axial reconstruction on the same patient demonstrating sustained uptake of [^{99m}Tc]MIBI in the region of suspected adenoma

metal' color scheme (see figures 1, 2). However, only the axial fused dataset was used for the purpose of this study.

Image review

Data were fully anonymized prior to review on a Barco Diagnostic Imaging monitor for blinded retrospective analysis. The datasets were jointly reviewed by two experienced consultant radio-nuclide radiologists and consensus was achieved. Reviewers were blinded to the timing of the axial SPECT/CT dataset and did not have access to patient history, laboratory results, or previous imaging.

Planar images and fused SPECT/CT axial reconstructions for each patient were initially reviewed separately. The reviewers determined whether each set of images was positive, negative, or indeterminate for the presence of a parathyroid adenoma. They then evaluated whether the diagnosis of a parathyroid adenoma was made via the planar images alone, the SPECT/CT alone independently or in a combination. Scans were classed as indeterminate when a definitive conclusion could not be reached. A two-alternative forced-choice strategy was employed whereby indeterminate scans were classed as negative.

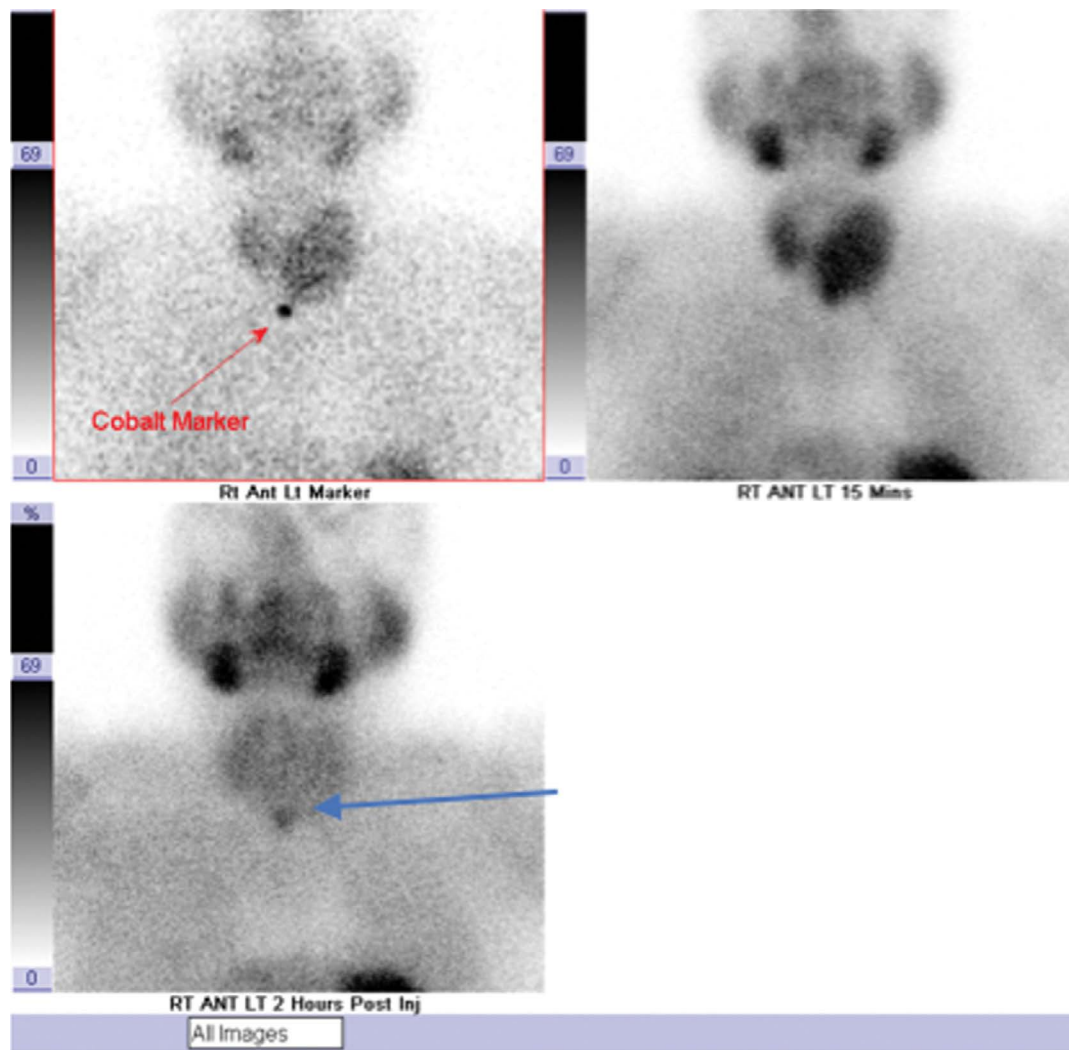


Figure 2. Planar parathyroid scintigraphy images in a patient with known multi-nodular goiter: Blue arrow indicates the presence of focally increased uptake which may represent a parathyroid adenoma or retained [^{99m}Tc]MIBI within a thyroid nodule

Statistical analysis

Data were input into a Microsoft EXCEL 2016 spreadsheet and Fisher's exact Chi-squared statistic was used to evaluate the diagnostic performances of early and late SPECT/CT and planar versus late SPECT/CT acquisition.

Results

Demographics and referral criteria

The sample population consisted of 36 patients, comprising 28 females (78%) and 8 males (22%). Age range was 24 to 83 years (mean = 59, SD 14.0).

Image analysis

In total, 21 likely parathyroid adenomas were identified within the patient sample, of which 13 were demonstrated on all sets of acquisitions. In the group comprising early planar and early SPECT/CT acquisitions:

- images were negative for the presence of parathyroid adenoma in 18 cases;
- four parathyroid adenomas were visualized on planar images only;
- one parathyroid adenoma was visualized on early SPECT/CT only;
- thirteen parathyroid adenomas were visualized on both early planar and SPECT/CT images (Tab. 2).

The Fisher's exact test found a significant difference between the diagnostic performance of early planar and SPECT/CT ($p < 0.001$). In the group consisting of late planar and SPECT/CT acquisitions:

- images were negative for the presence of parathyroid adenoma in 15 cases;
- six parathyroid adenomas were visualized on late SPECT/CT only;
- all 15 suspected parathyroid adenomas on planar images were also visualized on late SPECT/CT images (Tab. 3).

The Fisher's exact test found a significant difference between the diagnostic performance of late planar and SPECT/CT ($p < 0.001$).

Table 2. 2 × 2 contingency table comparing early planar and SPECT/CT diagnostic findings

		Early SPECT/CT		
		Negative	Positive	Total
Planar acquisition	Negative	18	1	19
	Positive	4	13	17
	Total	22	14	36

SPECT/CT — single-photon emission computed tomography/computed tomography

Table 3. 2 × 2 contingency table comparing late planar and SPECT/CT diagnostic findings

		Late SPECT/CT		
		Negative	Positive	Total
Planar acquisition	Negative	15	6	21
	Positive	0	15	15
	Total	15	21	36

SPECT/CT — single-photon emission computed tomography/computed tomography

Table 4. 2 × 2 contingency table comparing early and late SPECT/CT diagnostic findings

		Late SPECT/CT		
		Negative	Positive	Total
Early SPECT/CT	Negative	15	7	22
	Positive	0	14	14
	Total	15	21	36

SPECT/CT — single-photon emission computed tomography/computed tomography

Comparison of early and late SPECT/CT imaging protocols

Table 4 depicts the diagnostic performance of early and late SPECT/CT imaging protocols, with late SPECT/CT identifying an additional 7 adenomas not visualized within the early SPECT/CT dataset. All 14 suspected adenomas identified on early SPECT/CT were also visualized on late SPECT/CT images. The Fisher's exact test found a significant difference between the diagnostic performance of early and late SPECT/CT ($p < 0.001$).

Discussion

This study has demonstrated significantly superior performance of late-phase SPECT/CT in the identification of parathyroid adenomas with only 14 (67%) of the total of 21 suspected parathyroid adenomas demonstrated on early SPECT/CT alone.

Previous research has failed to define a single standardized imaging methodology for imaging of the parathyroid glands with evidence in support of both early and delayed SPECT/CT. Consequent implications for study duration and patient throughput underscore the need for a standardized, gold-standard, evidenced-based parathyroid imaging protocol.

Single-photon emission computed tomography/computed tomography (SPECT/CT) images have been found to be diagnostically superior to single or dual-phase planar or SPECT images [13]. Some centers perform SPECT/CT directly after early phase planar

acquisition while others perform SPECT/CT following late planar acquisition, typically two hours post [^{99m}Tc]MIBI administration. Late SPECT/CT has previously been proposed as the imaging methodology of choice for improved sensitivity in the detection of parathyroid adenomas [14].

All 14 adenomas identified on early SPECT/CT imaging were also apparent on an independent review of the late SPECT/CT images, therefore omission of the early SPECT acquisition would not have altered diagnosis within the study sample.

An additional six parathyroid adenomas were reported on a review of the late SPECT/CT images that had not been identified on the review of the planar images. These findings are consistent with previous studies demonstrating the added value of SPECT/CT over planar scintigraphy in the localization of parathyroid adenomas [13].

Figure 1A–C illustrate the importance of late imaging to assess delayed retention of [^{99m}Tc]MIBI indicating the presence of a parathyroid adenoma. Delayed planar imaging after thyroid washout illustrates a single area of retained, increased focal uptake of [^{99m}Tc]MIBI suggestive of a parathyroid adenoma.

In Figure 1B, there is an uptake of [^{99m}Tc]MIBI visualized in the thyroid on early SPECT/CT acquisition. There is potential for the visualized hotspot to represent a thyroid nodule, hindering definitive diagnosis. The additional delayed SPECT/CT image (Fig. 1C) demonstrates thyroid washout of [^{99m}Tc]MIBI with retained activity suggestive of a parathyroid adenoma.

[^{99m}Tc]MIBI negative images

The sensitivity of dual-phase parathyroid scintigraphy is limited in several instances including small lesion size, multiglandular disease, and co-existing thyroid disease. Consequently, a negative dual-phase [^{99m}Tc]MIBI scan does not exclude the presence of a parathyroid adenoma. False-negative, false-positive and indeterminate findings are well recognized [3]. Although all sample patients had clinical histories suggestive of parathyroid disease, only 58% (21/36) had likely parathyroid adenomas visualized on review of the acquired images. Surgical and pathology data were not collated, precluding sensitivity and specificity analyses.

The potential for thyroidal retention of [^{99m}Tc]MIBI particularly in the presence of concurrent thyroid disease may hinder the detection of parathyroid disease. Multi-modal imaging is of benefit to confirming or out rule the presence of a parathyroid adenoma in cases where thyroid disease limits the sensitivity of a single imaging modality [15]. One study patient had a notable multi-nodular goiter (Fig. 2), hindering diagnostic accuracy and underlining the limitations of parathyroid scintigraphy in this patient cohort. The sample size of 36 is relatively small however produced statistically significant results. Larger sample size would further validate the study findings.

Acquired images were reviewed concurrently with both radiologists working together rather than independently and any inter-observer variability was resolved via consensus agreement. The potential for inter-rater variability on an independent review of the images was not assessed. The implementation of a two-alternative forced-choice strategy resulted in nine indeterminate results being reclassified as negative, leading to a bias toward underdiagnosis.

The investigators had no access to the clinical history, laboratory results, pathology reports, surgical reports, official radiology reports, or further imaging undergone by the sample cohort. In the normal working environment, this information is readily available and provides increased accuracy of results within an informed clinical context.

Conclusions

We have demonstrated that delayed phase SPECT/CT is significantly superior to early SPECT/CT in the identification of likely parathyroid adenomas ($p < 0.001$). The reported potential for some parathyroid adenomas to show early washout of [^{99m}Tc]MIBI was not demonstrated.

An additional 6 likely parathyroid adenomas were identified on late SPECT/CT that was not reported on a review of the associated planar image acquisitions. Late SPECT/CT improves diagnostic accuracy over planar imaging alone ($p < 0.001$), consistent with prior research [13].

We have validated local imaging protocols and found that the practice of early (15 minutes) and late planar imaging, plus a single late phase SPECT/CT two hours post-administration of [^{99m}Tc]MIBI is the most accurate parathyroid scintigraphy protocol. This refined imaging protocol has been implemented within the Nuclear Medicine department at our institution. Elimination of the early SPECT/CT acquisition has obvious implications for decreased image processing time and storage space and reduced patient scan time by a minimum of 13 minutes, with increased patient throughput.

Conflict of interest

There are no conflicts of interest to declare.

References

1. Brown SJ, Ruppe MD, Tabatabai LS. The parathyroid gland and heart disease. *Methodist DeBakey Cardiovasc J.* 2017; 13(2): 49–54, doi: [10.14797/mdcj-13-2-49](https://doi.org/10.14797/mdcj-13-2-49), indexed in Pubmed: [28740581](https://pubmed.ncbi.nlm.nih.gov/28740581/).
2. Shindo M, Lee JA, Lubitz CC, et al. The changing landscape of primary, secondary, and tertiary hyperparathyroidism: highlights from the American College of Surgeons panel, "What's new for the surgeon caring for patients with hyperparathyroidism". *J Am Coll Surg.* 2016; 222(6): 1240–1250, doi: [10.1016/j.jamcollsurg.2016.02.024](https://doi.org/10.1016/j.jamcollsurg.2016.02.024), indexed in Pubmed: [27107975](https://pubmed.ncbi.nlm.nih.gov/27107975/).
3. Liddy S, Worsley D, Torreggiani W, et al. Preoperative imaging in primary hyperparathyroidism: literature review and recommendations. *Can Assoc Radiol J.* 2017; 68(1): 47–55, doi: [10.1016/j.carj.2016.07.004](https://doi.org/10.1016/j.carj.2016.07.004), indexed in Pubmed: [27681850](https://pubmed.ncbi.nlm.nih.gov/27681850/).
4. Kunstman JW, Udelsman R. Superiority of minimally invasive parathyroidectomy. *Adv Surg.* 2012; 46: 171–189, doi: [10.1016/j.yasu.2012.04.004](https://doi.org/10.1016/j.yasu.2012.04.004), indexed in Pubmed: [22873039](https://pubmed.ncbi.nlm.nih.gov/22873039/).
5. Chan RK, Ruan DT, Gawande AA, et al. Surgery for hyperparathyroidism in image-negative patients. *Arch Surg.* 2008; 143(4): 335–337, doi: [10.1001/archsurg.143.4.335](https://doi.org/10.1001/archsurg.143.4.335), indexed in Pubmed: [18427019](https://pubmed.ncbi.nlm.nih.gov/18427019/).
6. Minisola S, Cipriani C, Diacinti D, et al. Imaging of the parathyroid glands in primary hyperparathyroidism. *Eur J Endocrinol.* 2016; 174(1): D1–D8, doi: [10.1530/EJE-15-0565](https://doi.org/10.1530/EJE-15-0565), indexed in Pubmed: [26340967](https://pubmed.ncbi.nlm.nih.gov/26340967/).
7. Hindí E, Ugur O, Fuster D, et al. 2009 EANM parathyroid guidelines. *Eur J Nucl Med Mol Imaging.* 2009; 36(7): 1201–1216, doi: [10.1007/s00259-009-1131-z](https://doi.org/10.1007/s00259-009-1131-z), indexed in Pubmed: [19471928](https://pubmed.ncbi.nlm.nih.gov/19471928/).
8. Caveny SA, Klingensmith WC, Martin WE. Parathyroid imaging: the importance of dual-radiopharmaceutical simultaneous acquisition with ^{99m}Tc-sestamibi and ¹²³I. *J Nuclear Med Technol.* 2012; 40(2): 104–110, doi: <https://doi.org/10.2967/jnmt.111.098400>.
9. Erbil Y, Barbaros U, Yanik BT, et al. Impact of gland morphology and concomitant thyroid nodules on preoperative localization of parathyroid adenomas. *Laryngoscope.* 2006; 116(4): 580–585, doi: [10.1097/01.MLG.0000203411.53666.AD](https://doi.org/10.1097/01.MLG.0000203411.53666.AD), indexed in Pubmed: [16585862](https://pubmed.ncbi.nlm.nih.gov/16585862/).
10. Martin WH, Sandler MP, Gross MD. Thyroid, parathyroid, and adrenal gland imaging. In: Sharp PF, Gemmell HG, Murray DM. ed. *Practical Nuclear Medicine 3rd edition.* Springer, London 2005: 247–272.
11. Payne SJ, Smucker JE, Bruno MA, et al. Radiographic evaluation of non-localizing parathyroid adenomas. *Am J Otolaryngol.* 2015; 36(2): 217–222, doi: [10.1016/j.amjoto.2014.10.036](https://doi.org/10.1016/j.amjoto.2014.10.036), indexed in Pubmed: [25465322](https://pubmed.ncbi.nlm.nih.gov/25465322/).
12. Monzen Y, Tamura A, Okazaki H, et al. SPECT/CT fusion in the diagnosis of hyperparathyroidism. *Asia Ocean J Nucl Med Biol.* 2015; 3(1): 61–65, indexed in Pubmed: [27408883](https://pubmed.ncbi.nlm.nih.gov/27408883/).
13. Lavelly WC, Goetze S, Friedman KP, et al. Comparison of SPECT/CT, SPECT, and planar imaging with single- and dual-phase (^{99m}Tc)-sestamibi parathyroid scintigraphy. *J Nucl Med.* 2007; 48(7): 1084–1089, doi: [10.2967/jnumed.107.040428](https://doi.org/10.2967/jnumed.107.040428), indexed in Pubmed: [17574983](https://pubmed.ncbi.nlm.nih.gov/17574983/).
14. Qiu ZL, Wu Bo, Shen CT, et al. Dual-phase (^{99m}Tc)-MIBI scintigraphy with delayed neck and thorax SPECT/CT and bone scintigraphy in patients with primary hyperparathyroidism: correlation with clinical or pathological variables. *Ann Nucl Med.* 2014; 28(8): 725–735, doi: [10.1007/s12149-014-0876-z](https://doi.org/10.1007/s12149-014-0876-z), indexed in Pubmed: [25120244](https://pubmed.ncbi.nlm.nih.gov/25120244/).
15. Hwang SH, Rhee Y, Yun M, et al. Usefulness of SPECT/CT in parathyroid lesion detection in patients with thyroid parenchymal Tc-sestamibi retention. *Nucl Med Mol Imaging.* 2017; 51(1): 32–39, doi: [10.1007/s13139-016-0438-5](https://doi.org/10.1007/s13139-016-0438-5), indexed in Pubmed: [28250856](https://pubmed.ncbi.nlm.nih.gov/28250856/).